NASA TN D-1120

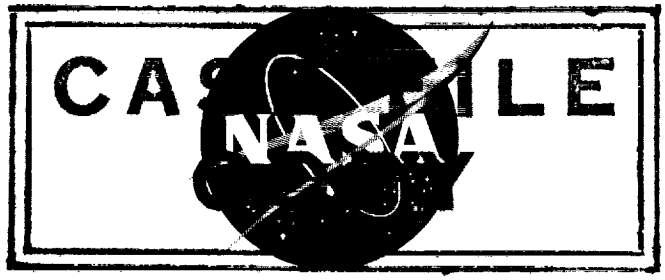

TECHNICAL NOTE

D-1120

SERVO LOOP DESIGN FOR AIR BEARING INERTIAL COMPONENTS

By Herman E. Thomason

George C. Marshall Space Flight Center
Huntsville, Alabama

NATIONAL AERONAUTICS AND SPACE ADMINISTRATION

WASHINGTON May 1962

NATIONAL AERONAUTICS AND SPACE ADMINISTRATION

TECHNICAL NOTE D-1120

SERVO LOOP DESIGN FOR AIR BEARING INERTIAL COMPONENTS

By Herman E. Thomason

SUMMARY

The analytical problems encountered in designing the electronics for air bearing inertial components are treated both by classical and transform methods. Extensive use is made of Laplace transformations, Nyquist and Bode analysis. Results from these several methods are presented in the form of graphs and plots where appropriate in the text.

A functional discussion of the various electronic subassemblies points out where the major mechanization problems occur. These problems are treated in sequence as they arise in the servo loop starting at the transducers and ending at the torquers. In each instance the design considerations, including the major problem areas and their practical solutions, are presented.

DISCUSSION

There are two types of servo loop amplifiers used with the MSFC inertial platform systems. One type of amplifier is used for stabilizing the air bearing gyro inertial reference loops; the other is used to stabilize the air bearing accelerometer loops. The major difference between the loops is that in the accelerometer loop an actual precession angle is required as a measure of vehicle velocity change; whereas in the inertial reference loop a nulling mode is used to hold the platform space-fixed. It can be shown that the electronics of the two loops are similar. Therefore, this discussion will only cover the electronics associated with the inertial reference loop.

Assuming small angular motions, the equations which describe the stabilizing loop can be formulated from FIGURE 1, which represents one axis of the platform. Applying Newton's Law in rotational form yields the following equations:

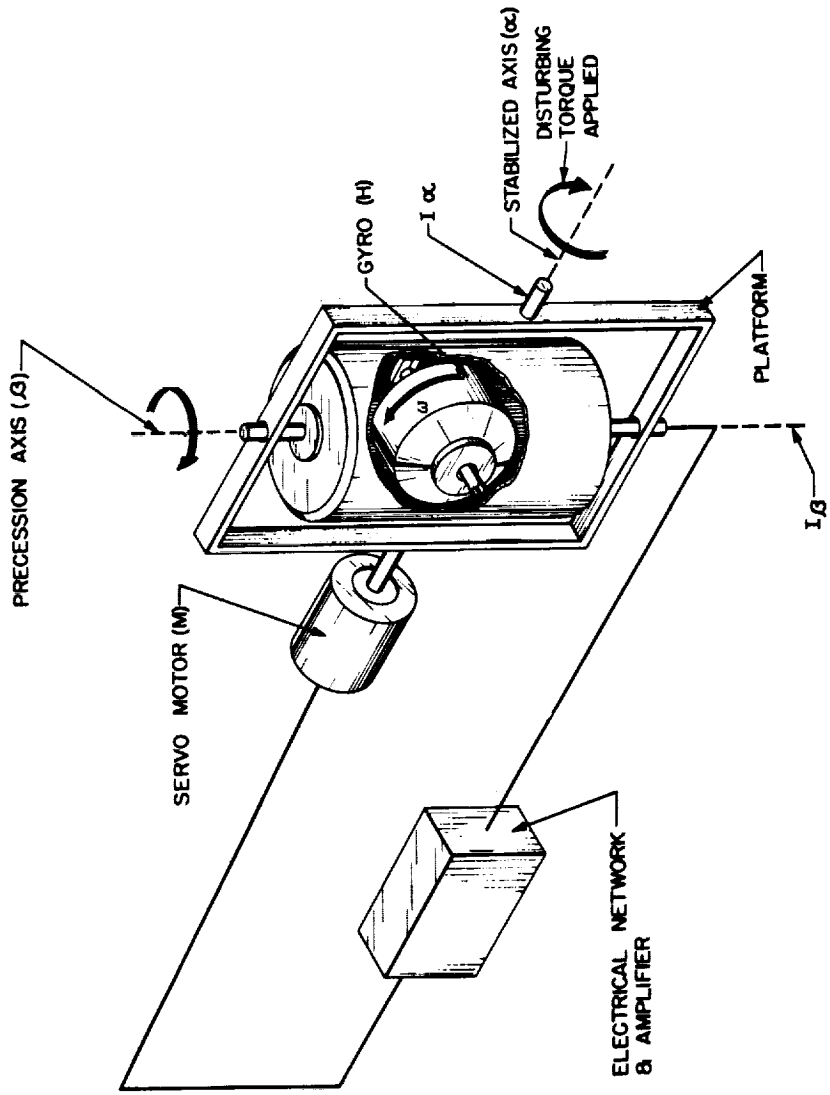

FIGURE 1. SINGLE AXIS GEOMETRY

$$T_d - T_m = J_\alpha \frac{d^2\alpha}{dt^2} + H_z \frac{d\beta}{dt} \quad (1)$$

$$T_\beta = J_\beta \frac{d^2\beta}{dt^2} - H_z \frac{d\alpha}{dt} \quad (2)$$

where T_d = disturbance torque

T_m = recovery torque (from servo motor)

J_α = platform moment of inertia about the stabilized axis

J_β = gyro moment of inertia about the air bearing axis

H_z = angular momentum of the gyro wheel (assumed constant)

α = inertial reference angle measured about the stabilized axis

β = precession angle measured about the air bearing axis

T_β = torques about the air bearing axis.

For the stability analysis purposes, the torque T_β is considered to be essentially zero because of the air bearing. Therefore, Equations 1 and 2 may be rewritten and put into Laplace transform notation as follows:

$$\bar{T}_d(s) - \bar{T}_m(s) = J_\alpha s^2 \bar{\alpha}(s) + H_z s \bar{\beta}(s) \quad (3)$$

$$0 = J_\beta s^2 \bar{\beta}(s) - H_z s \bar{\alpha}(s) \quad (4)$$

which can be rearranged to yield the following equations.

$$\bar{T}_d(s) - \bar{T}_m(s) = \frac{J_\alpha J_\beta}{H_z} s^3 \bar{\beta}(s) + H_z s \bar{\beta}(s) \quad (5)$$

$$\bar{\alpha}(s) = \frac{J_\beta}{H_z} s \bar{\beta}(s) \quad (6)$$

A block diagram of the loop based on these equations is illustrated in FIGURE 2.

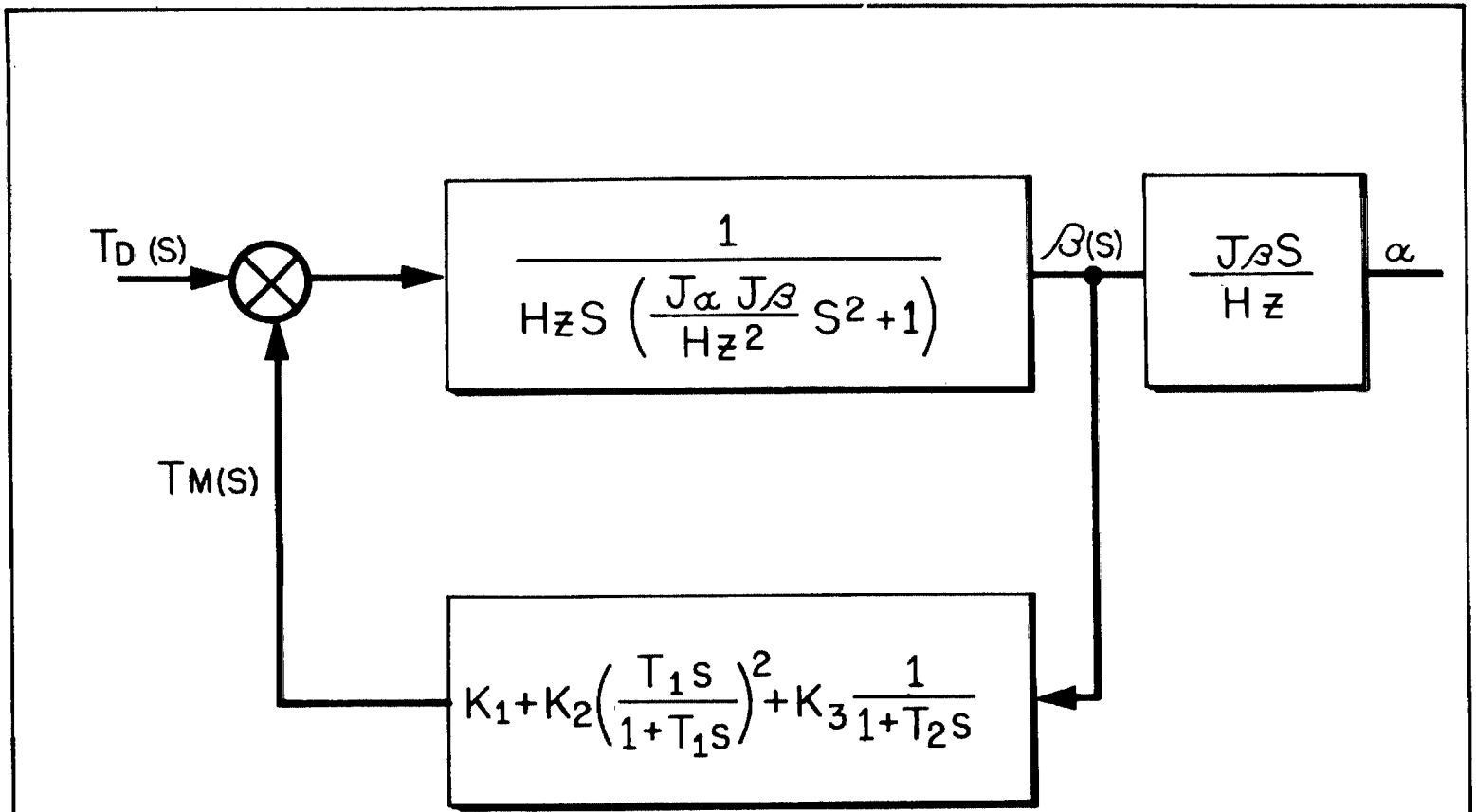

FIGURE 2. SINGLE AXIS BLOCK DIAGRAM WITH APPROXIMATION TO THE ELECTRONIC AMPLIFIER INCLUDED

Stabilization of the platform in the presence of disturbing influences is of primary interest. Therefore, an investigation of the response of the gyro precession angle, β, when a disturbing torque, T_d, is applied to the stabilized axis is a logical beginning point. The dynamic relationship between precession torque, with no corrective servo loop, is given by the following equation:

$$\frac{\bar{\beta}(s)}{\bar{T}_d(s)} = \frac{1}{J_\alpha J_\beta / H_z \; s \; (s^2 + H_z^2 / J_\alpha J_\beta)} \tag{7}$$

This indicates borderline stability and hence is unacceptable. To illustrate, suppose an impulse function of input torque (T_d) is applied. It will produce a time response of the form

$$K \sin \frac{H_z^2}{J_\alpha J_\beta} t$$ (note that this neither increases nor decreases with time and that the magnitude is proportional to the energy contained in the initial shock). This condition can be simulated in the laboratory by applying a shock about one of the stabilized axis of the platform with the servo loop de-energized. It can be observed from such a test that, although a cissoidal response results, it is not a completely undamped sinusoid as is indicated in the equation above. Therefore, in actuality, a small damping term should be associated with the time function in order to more accurately describe the mechanical portion of the system. A transfer function of the form

$$\frac{\bar{\beta}(s)}{\bar{T}_d(s)} = \frac{1}{\frac{J_\alpha J_\beta}{H_z} \; s \; (s^2 + Ds + H_z^2 / J_\alpha J_\beta)}$$

would, therefore, be more realistic. The damping constant "D" results from unavoidable gear friction, bearing friction, and other losses between gimbals of the platform. This damping term plays an important role in the platform stability realization. A Nyquist plot of these mechanical characteristics combined with the servo loop characteristics will illustrate the importance of this damping constant. The servo amplifier characteristics are presented in the form of a phase and amplitude plot in FIGURE 3. A Nyquist plot of the system characteristics without mechanical friction is shown in FIGURE 4 and is labeled No. 2. This plot reveals a discontinuity at approximately 5.8 cps producing an infinite amplitude and a phase reversal of 180°. This is caused by the undamped quadratic $(s^2 + H_z^2 / J_\alpha J_\beta)$. This plot crosses the 180° line twice. First with an amplitude greater than one and then, at a higher frequency, with an amplitude less than one.

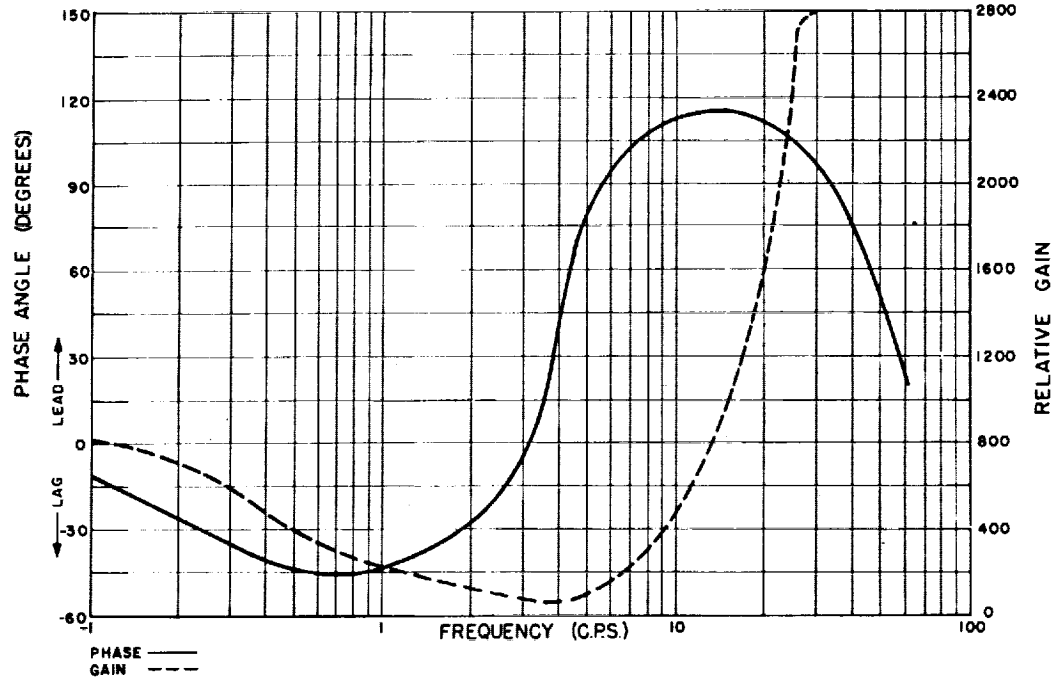

FREQUENCY RESPONSE OF ACCELEROMETER AMPLIFIER
(Phase Angle & Gain vs Frequency)

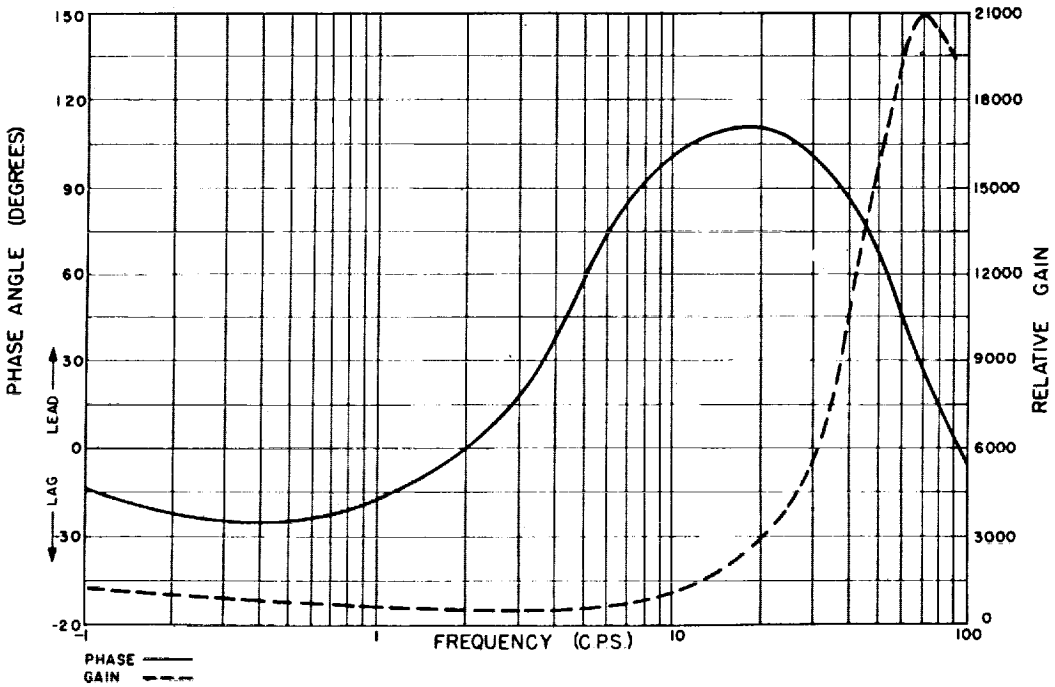

FIGURE 3. FREQUENCY RESPONSE OF STABILIZING AMPLIFIER
(PHASE ANGLE & GAIN VERSUS FREQUENCY)

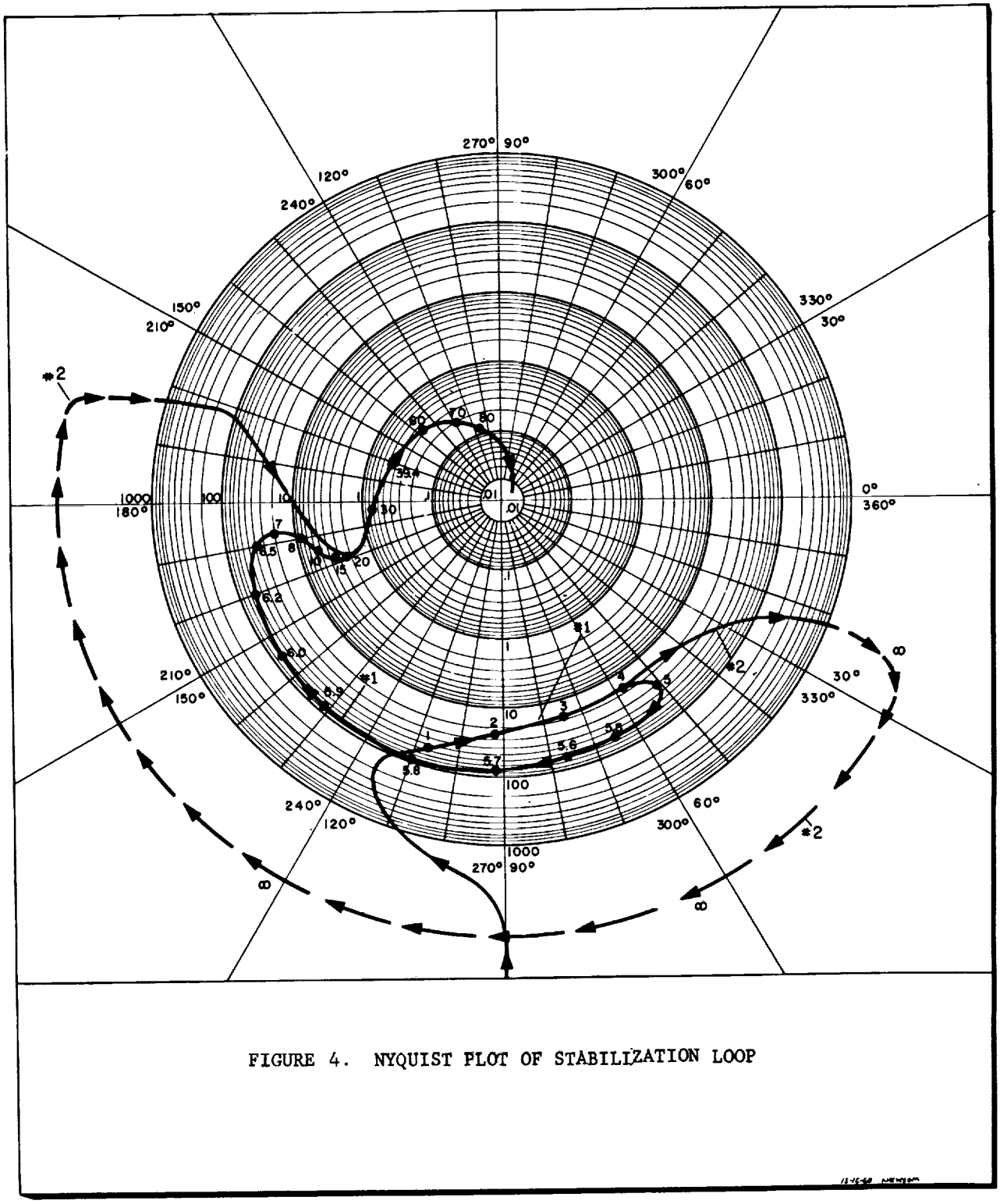

FIGURE 4. NYQUIST PLOT OF STABILIZATION LOOP

This indicates a conditionally stable system which may become unstable either with a gain setting too low or too high. It can be seen from this plot that in order to avoid this condition the electronics must produce at least enough phase shift to bring the plot above the positive real axis prior to the point of discontinuity. Fortunately, the small mechanical damping helps to minimize this condition as is shown on Nyquist plot curve No. 1. This shows that the infinite discontinuity does not exist and the negative real axis of the Nyquist plot is not reached prior to the loop gain reaching unity magnitude. This mechanical damping is present to a much smaller degree in the accelerometer loops. Thus the accelerometer loop electronics have to furnish almost all the damping necessary to stabilize the loop. This greatly magnifies the difficulty in stabilizing the accelerometer loop which is actually a conditionally stable one in practice.

The equation for the closed loop system response is:

$$\frac{\bar{\beta}(s)}{\bar{T}_d(s)} = \frac{1}{\frac{J_\alpha J_\beta}{H_z} s^3 + H_z s + G(s)} \tag{8}$$

where G(s) is a function operating on the β angle (gyro precession angle) to produce a servo motor torque, T_m, in conjunction with the servo amplifier electronics. In order to achieve stability in this system, $\bar{T}_m(s)$ must at least contain terms of the form $(K_1 s^2 + K_2)$. This minimum requirement results in the following equation:

$$\frac{\bar{\beta}(s)}{\bar{T}_d(s)} = \frac{1}{J_\alpha\, J_\beta/H_z \quad s^3 + K_1 s^2 + H_z s + K_2} \tag{9}$$

which possesses the necessary although not necessarily sufficient conditions for stability. In a demodulate, equalize, remodulate scheme, dc compensation is used in the electronics to realize the necessary terms. FIGURE 5 shows the servo amplifier broken into its functional parts. The frequency concept of the system focuses attention to the Bode plot (FIG. 6) and its attendant techniques to obtain satisfactory approximations.

The pick-off or transducer, which is used to measure the precession angle β, is a shorted turn inductive type using a 400 cps ac carrier excitation voltage. A detailed sketch of this device is shown in FIGURE 7.

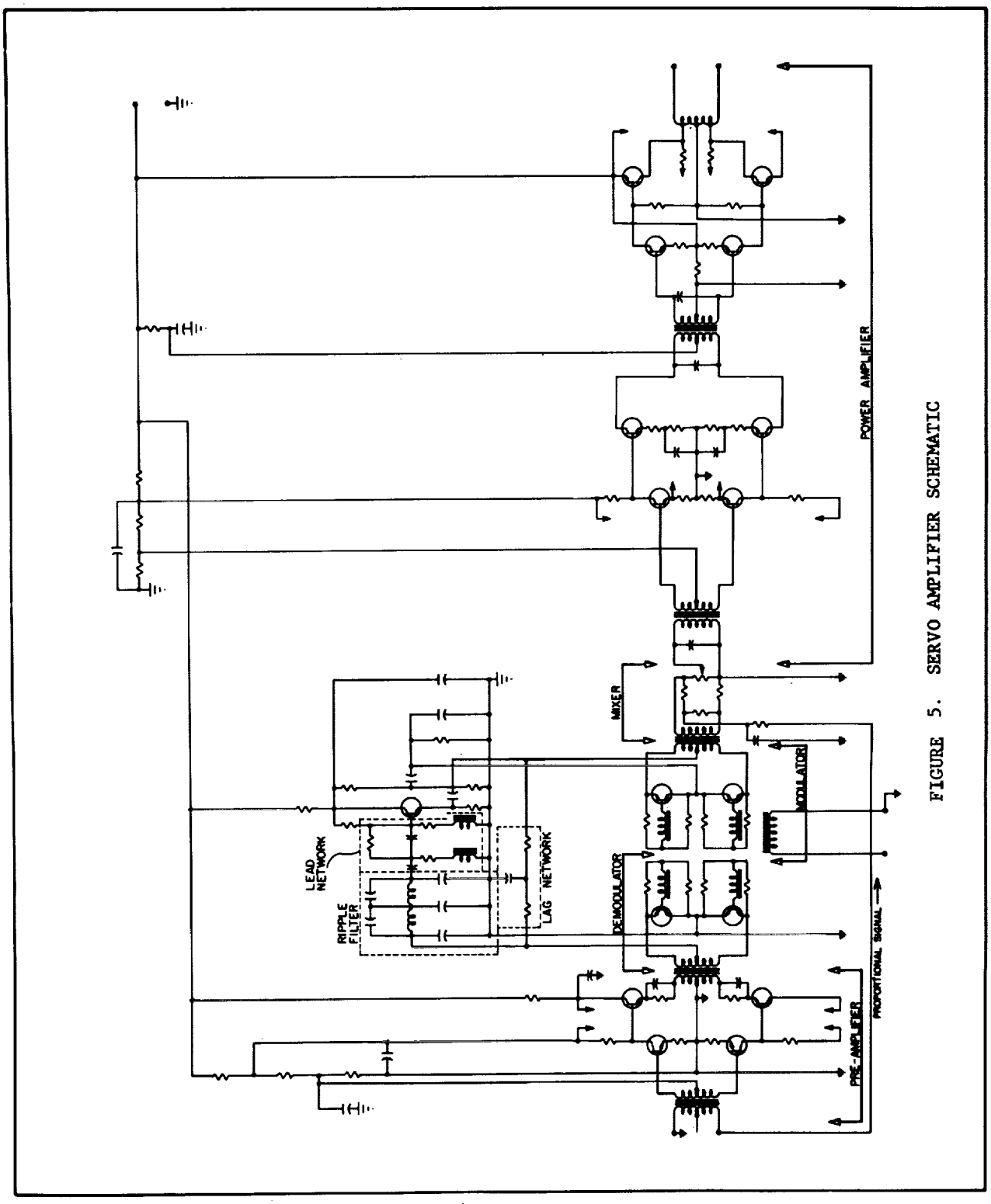

FIGURE 5. SERVO AMPLIFIER SCHEMATIC

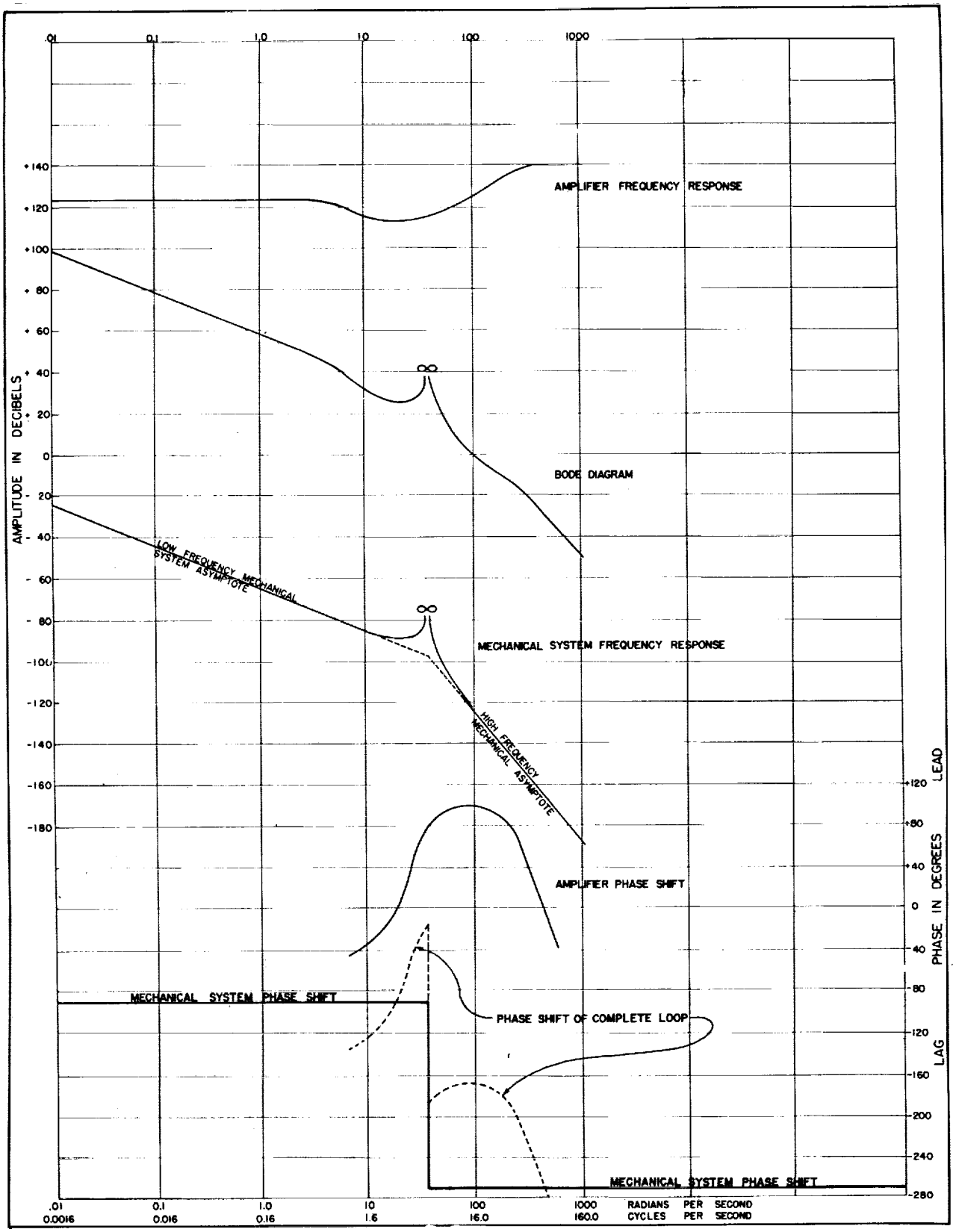

FIGURE 6. FREQUENCY RESPONSE AND BODE PLOT OF ST-120 SYSTEM

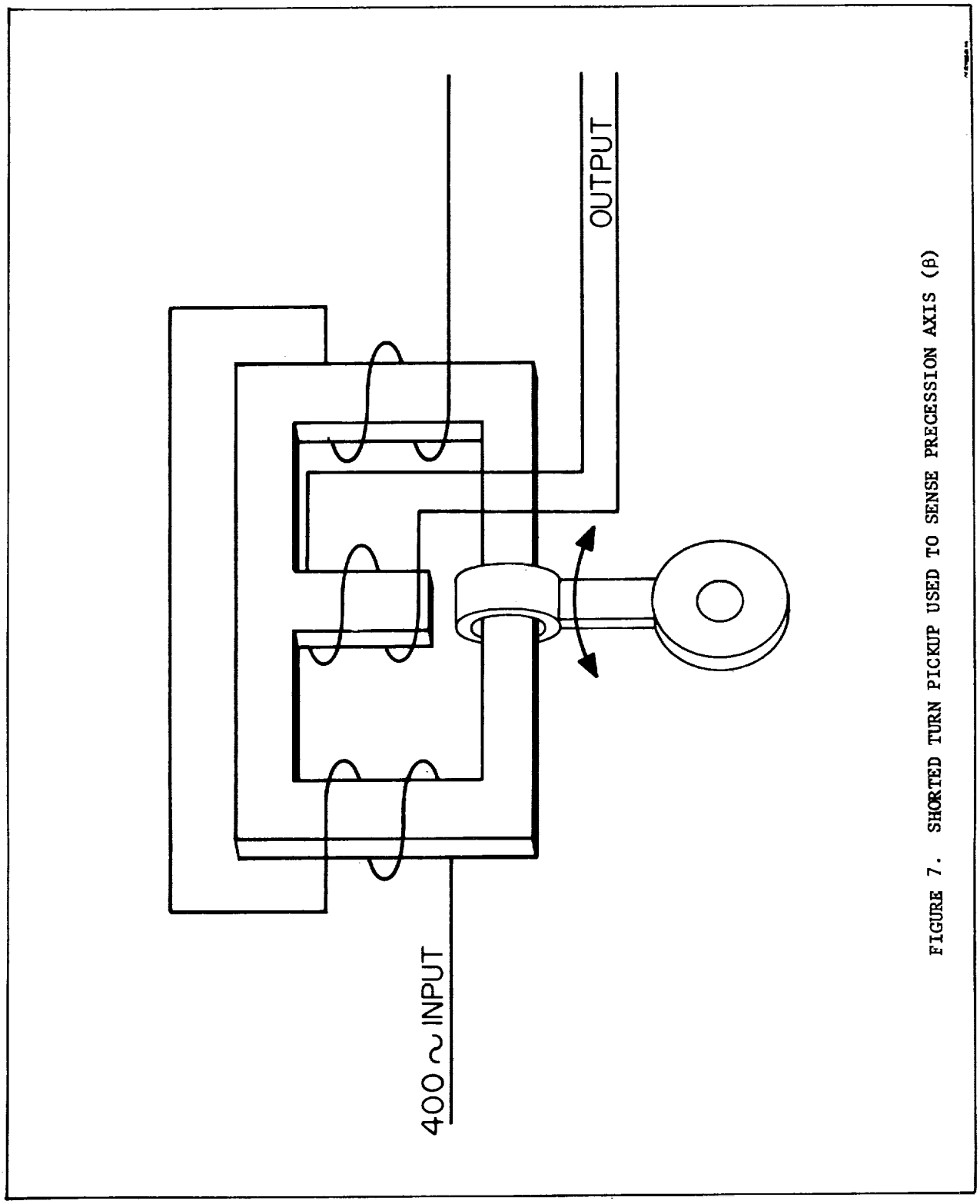

FIGURE 7. SHORTED TURN PICKUP USED TO SENSE PRECESSION AXIS (β)

In operation an excitation voltage is applied to the two windings on the outside of the iron core. These windings are phased so that the two flux patterns are additive along the periphery, but are opposing in the center leg. A solid copper loop is placed around the outside portion of the core which connects the outer legs. The shorted turn is attached to the floated can and is free to move when the gyro precesses. Theoretically, when this shorted turn is in the center of its travel, the flux from the two outside windings are equal and opposite in the center leg and no voltage is induced in the output coil. When the shorted turn moves to either side of this center position, the flux in the center becomes unbalanced and a voltage is induced in the output. The voltage is proportional in magnitude to the displacement of the shorted turn and is either in phase or 180° out of phase, depending on the direction of travel, with the excitation voltage. The output voltage is reasonably linear for deflections between one tenth of a degree and three degrees. In the vicinity of the null or center position there is a residual quadrature component which causes a small null voltage. Magnetic effects also exert a tractive force on the shorted turn unless the pick-off load is set to an optimum value. For this reason, the sensitivity of the pick-off is limited to a few millivolts per degree.

The low sensitivity of the pick-off necessitates that the transducer voltage be amplified before detection. This preamplifier, indicated in FIGURE 5, uses two transistor stages and has a voltage gain of approximately forty. It has a low output impedance in order to drive the demodulator. The input impedance is set to a predetermined value for minimizing the effects of reaction torque.

The demodulator is a phase sensitive circuit employing symmetrical transistors. FIGURE 5 includes a schematic diagram of the demodulator. A 400 cps excitation voltage is used to "key" or switch the two demodulator transistors through separate secondary windings from a common transformer. The secondary windings are phased such that when one transistor is conducting, the other is shut off. The keying voltage has identical zero crossings to the input voltages from the preamplifier so that the output voltage from the demodulator is a full wave demodulated signal. The polarity is dependent upon the phasing of primary voltage of the keying transformer and hence to the sign of β, the precession angle. The demodulator is a potential source of noise in the amplifier. Therefore, the signal is maintained at as high a level as possible to remain consistent with transistor voltage limitations. The maximum gain from the pick-off to the demodulator input is set so that, for maximum pick-off output, the voltage input to the demodulator is approximately 20 volts from zero to peak. This voltage is limited by the amount of signal current the ripple filter can absorb without saturating as well as by the maximum voltage the transistors can withstand in the reverse direction. The higher the signal level that can be accommodated prior to demodulation, the better the signal to noise ratio in the output.

The demodulated output must be filtered to remove the ripple which would saturate the lead equalization circuitry. A filter is inserted after the output of the demodulation as shown in FIGURE 5. The waveform to be filtered is a full wave signal with the amplitude proportional to the displacement of the pick-up. A Fourier series expansion of this wave reveals the frequency response which will be required of the filter.

$$f(\omega t) = \frac{2A}{\pi}\left(1 - \frac{2\cos 2\omega t}{3} - \frac{2\cos 4\omega t}{15} - \frac{2\cos 6\omega t}{35}\right)$$

where $\omega = 2\pi f = 2\pi\ (400)$

A = amplitude proportional to "β" (the precession angle).

The dc term in this expansion carries the desired information about the pick-up displacement; therefore, ideally, the filters should reject all the harmonics. In practice it is not possible to reject all harmonics completely; however, by looking at the relative strengths of the different components it is seen that the second and fourth carry over 80% of the harmonic power. A filter which attenuates these harmonics sufficiently while passing frequencies of at least 100 cps without significant attenuation is adequate. FIGURE 8 is a plot of the frequency response of the filter now being used. The attenuation is greatest (about 33 db) for 800 cps, the second harmonic, and is down almost as low for 400 cps. Phase shift for frequencies below 100 cps is the main difficulty introduced by the ripple filter. For instance, a lag of 75 degrees is present at 100 cps. This lag must be compensated for by the lead networks following the ripple filter in order to have a highly damped system. Considerable effort has been expended trying to realize what amounts to an ideal low pass filter. Various other filter configurations have been tried but these filters do not have enough attenuation at 1600 cps (4th harmonics).

The ripple filter output is introduced into another filter section, which is termed the lead network. It is this section of the amplifier that has required the most attention. Numerous schemes have been tried in synthesizing this section. Earlier it was pointed out that the servo amplifier must at least generate terms of the form $K_1 S^2 + K_2$. Theoretically these terms could be generated by two simple RC stages. It has been found that, with this type of network, the component values are too critical and the attenuation too great to be practical. Therefore, RLC networks are used which are terminated in an emitter follower stage (FIG. 5). The phase shift realized by this network in the frequency range of interest goes as high as 150 degrees lead; however, it also attenuates the signal as much as 60 db at low frequencies.

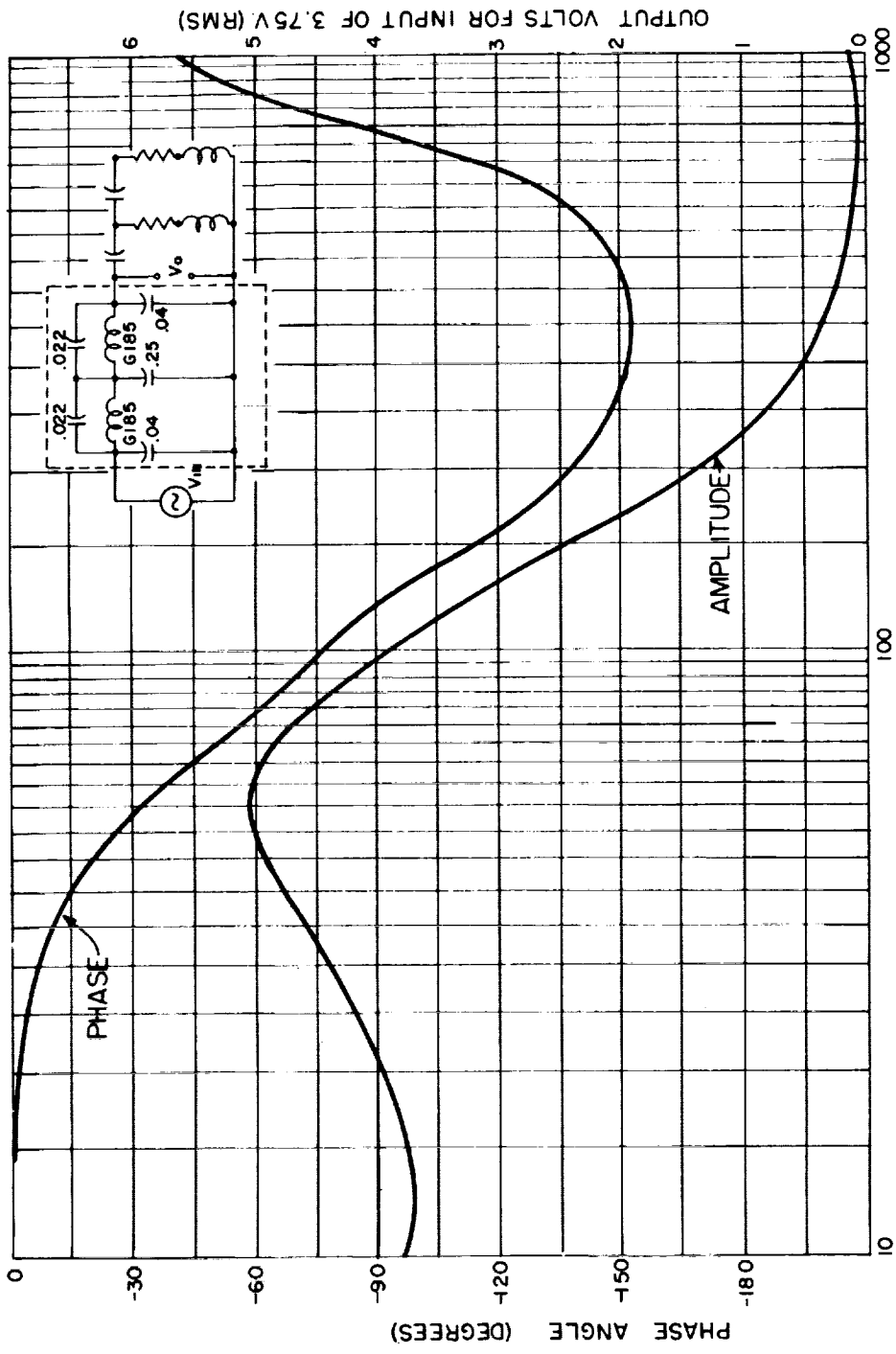

FIGURE 8. PHASE AMPLITUDE PLOT FOR RIPPLE FILTER

This attenuation causes the noise problem to be critical, since lead networks inherently accentuate any high frequency noise present in the desired signal. Although these networks appear to give satisfactory results, it is felt that the maximum amount of compensation has been realized using this configuration and further significant improvements will have to come from other sources such as broad banding the amplifier and/or using dc torquers. The servo amplifier characteristics for both the stabilizing and accelerometer loops are presented in FIGURE 3.

A portion of the amplifier which was not mentioned previously in the theory is the lag network. This network is a simple low pass RC filter (FIG. 5). The transfer function for this network may be written:

$$\frac{E_o}{E_1} = \frac{R_o}{R^2_c} \quad \frac{1}{S + 2/RC} \quad \text{assuming } R \gg R_o$$

where R_o = load resistance

which has the form of a simple low pass filter with break frequency at 2/RC radians. Ideally, the lag network will increase the dc gain of the system while not affecting the damping. This is accomplished by adjusting the break frequency so that signals at frequencies above about 0.1 cps will not be passed through this section.

The signal from the lead network and the lag network are mixed together as shown in FIGURE 5 and then applied to the chopper. The chopper or modulator is identical in form to the demodulator (FIG. 5) and performs the function of remodulating the signal into a 400 cps carrier system. The dc signal from the lead-lag networks is applied to the modulator input through a transformer. The keying voltage is taken from the same transformer as for the demodulator. This voltage alternately switches the transistors on and off at 400 cps, thus drawing current through the primary of the modulator transformer first in forward direction and then in reverse direction. This causes the signal to be modulated.

The modulator operates at a very low signal level as well as a low signal to noise ratio. This is because the differentiation process in the lead network tends to accentuate any distortion in the signal and also passes, with little or no attenuation, all the harmonics generated by the demodulator process which are not rejected by the ripple filter. Because the modulator does operate at a low signal level, many of the problems of the servo system can be traced to this area. High temperature effects on the modulator transistors have been found to cause instability in the platform system unless silicon transistors are used. Another undesirable effect is the small amount of leakage of the 400 cps keying voltage into the output. This is due to nonuniformity in

the transistors and is particularly troublesome in the accelerometer amplifier since it can affect the precession rate. To compensate for this effect, a signal is inserted with the proper phase to cancel the signal leaking through the modulator transistors.

All amplifiers make use of a hybrid mixer for combining the output from the modulator with the proportional signal (FIG. 5). This circuit has the advantage of isolating the inputs, but the disadvantage of reducing the output by a factor of two. For best results the resistors should be large enough not to load the modulator; however, they must be considerably lower than the input impedance of the power amplifier to avoid loading effects.

The power amplifier receives the combined signal from the mixer and raises it to a power level sufficient to drive the ac torque motor. This amplifier is a four stage, push-pull, transistor amplifier capable of a minimum output of five watts. The push-pull arrangement has the advantage of canceling even harmonics thereby reducing output distortion and also is less influenced by power supply interaction between stages.

NASA TN D-1120
National Aeronautics and Space Administration.
SERVO LOOP DESIGN FOR AIR BEARING INERTIAL COMPONENTS. Herman E. Thomason. May 1962. 16p. OTS price, $0.50.
(NASA TECHNICAL NOTE D-1120)

This report is a comprehensive discussion of the problems, both analytical and practical, encountered in designing the electronics for air bearing inertial components. The analytical problems are treated both by classical and transform methods. Extension use is made of Laplace transformations, Nyquist and Bode analysis. Results from these several methods are presented in the form of graphs and plots where appropriate in the text. A functional discussion of the various electronic subassemblies points out where the major mechanization problems occur. These problems are treated in sequence as they arise in the servo loop starting at the transducers and ending at the torquers. In each instance the design considerations, including the major problem areas and their practical solutions, are presented.

I. Thomason, Herman E.
II. NASA TN D-1120

(Initial NASA distribution:
22, Guidance and homing systems;
27, Mathematics;
32, Physics, solid state;
51, Stresses and loads;
52, Structures.)

NASA

NASA TN D-1120
National Aeronautics and Space Administration.
SERVO LOOP DESIGN FOR AIR BEARING INERTIAL COMPONENTS. Herman E. Thomason. May 1962. 16p. OTS price, $0.50.
(NASA TECHNICAL NOTE D-1120)

This report is a comprehensive discussion of the problems, both analytical and practical, encountered in designing the electronics for air bearing inertial components. The analytical problems are treated both by classical and transform methods. Extension use is made of Laplace transformations, Nyquist and Bode analysis. Results from these several methods are presented in the form of graphs and plots where appropriate in the text. A functional discussion of the various electronic subassemblies points out where the major mechanization problems occur. These problems are treated in sequence as they arise in the servo loop starting at the transducers and ending at the torquers. In each instance the design considerations, including the major problem areas and their practical solutions, are presented.

I. Thomason, Herman E.
II. NASA TN D-1120

(Initial NASA distribution:
22, Guidance and homing systems;
27, Mathematics;
32, Physics, solid state;
51, Stresses and loads;
52, Structures.)

NASA

NASA TN D-1120
National Aeronautics and Space Administration.
SERVO LOOP DESIGN FOR AIR BEARING INERTIAL COMPONENTS. Herman E. Thomason. May 1962. 16p. OTS price, $0.50.
(NASA TECHNICAL NOTE D-1120)

This report is a comprehensive discussion of the problems, both analytical and practical, encountered in designing the electronics for air bearing inertial components. The analytical problems are treated both by classical and transform methods. Extension use is made of Laplace transformations, Nyquist and Bode analysis. Results from these several methods are presented in the form of graphs and plots where appropriate in the text. A functional discussion of the various electronic subassemblies points out where the major mechanization problems occur. These problems are treated in sequence as they arise in the servo loop starting at the transducers and ending at the torquers. In each instance the design considerations, including the major problem areas and their practical solutions, are presented.

I. Thomason, Herman E.
II. NASA TN D-1120

(Initial NASA distribution:
22, Guidance and homing systems;
27, Mathematics;
32, Physics, solid state;
51, Stresses and loads;
52, Structures.)

NASA

NASA TN D-1120
National Aeronautics and Space Administration.
SERVO LOOP DESIGN FOR AIR BEARING INERTIAL COMPONENTS. Herman E. Thomason. May 1962. 16p. OTS price, $0.50.
(NASA TECHNICAL NOTE D-1120)

This report is a comprehensive discussion of the problems, both analytical and practical, encountered in designing the electronics for air bearing inertial components. The analytical problems are treated both by classical and transform methods. Extension use is made of Laplace transformations, Nyquist and Bode analysis. Results from these several methods are presented in the form of graphs and plots where appropriate in the text. A functional discussion of the various electronic subassemblies points out where the major mechanization problems occur. These problems are treated in sequence as they arise in the servo loop starting at the transducers and ending at the torquers. In each instance the design considerations, including the major problem areas and their practical solutions, are presented.

I. Thomason, Herman E.
II. NASA TN D-1120

(Initial NASA distribution:
22, Guidance and homing systems;
27, Mathematics;
32, Physics, solid state;
51, Stresses and loads;
52, Structures.)

NASA